DEVELOPING THE COMBINED KALMAN-EMD ALGORITHM TO PROCESS BLASTING SHOCKWAVE SIGNALS PROPAGATING IN A WATER MEDIUM

Tung Lam Vu[1,*], Duc Viet Tran[2], Ngoc Lam Bui[3], Trong Thang Dam[1]

[1]*Institute of Techniques for Special Engineering, Le Quy Don Technical University, Hanoi, Vietnam*

[2]*General Department of Defence Industry, Hanoi, Vietnam*

[3]*X28 Factory, Haiphong, Vietnam*

Abstract

In experiments deploying underwater blast sensors, measured data is always disturbed, expressed as analog peaks in the obtained signal form. Except for pressure peak p_{max}, other parameters of an underwater explosion such as positive impulse I^+, positive phase duration τ^+, negative impulse I^- and negative phase duration τ^- are difficult or almost impossible to extract from this signal type. This article studies developing an algorithm called Kalman-EMD with the combination of Kalman filter and empirical mode decomposition for processing this signal type. The algorithm is applied in 6 data sets measuring the shockwave pressure of underwater explosions by PCB W138A05 sensors with the same condition that 184 grams of A-IX-2 explosive is detonated underwater. The results show that noise in signals is significantly eliminated. For the blasting parameters of processed signals, which can be compared with theory such as I^+ and τ^+, although it witnesses a small trade-off when errors of I^+ enhance from about 3% to 6%, errors of τ^+ are significantly decreased from about over 30% to only about 3%. Especially other pieces of information, such as I^- and τ^- can be extracted from the processed signal, so this trade-off can be acceptable. Hence, this algorithm can be applied to denoise and extract parameters from shockwave pressure signals of underwater explosions.

Keywords: *Underwater explosions (UNDEX); denoising; Empirical mode decomposition (EMD); Kalman filter.*

1. Introduction

Explosive energy has been widely used both in the world and in Vietnam to save costs and time. Still, the explosive efficiency of the best explosives today has only about 20% of the explosive energy becoming effective power to break soil and rocks [1, 2], the rest of that transforms into heat and vibration, affecting the surrounding environment. Controlling explosive energy to destroy objects at will while limiting negative impacts on the surrounding environment is an important research area in the blasting work.

*Email: lamvt@lqdtu.edu.vn

DOI: 10.56651/lqdtu.jst.v7.n01.833.sce

The research direction inclined to analyze the dynamic effects of the blasting load, which is expressed by the parameters of the explosion, is one of the aforementioned solutions above. Many scientists in the world and Vietnam have researched in this direction. Typically, the research of author D. T. Thang et al. [3-5] conducted numerous experiments measuring many parameters of the explosion, including underwater shockwave pressure. However, there are several reasons [6] leading to distortion of the original waveform, obscuring important characteristics of the explosion signal, and making it difficult to further analyze.

Fortunately, there are several denoising methods proposed by scientists. Filtering algorithms such as Empirical Mode Decomposition (EMD), Ensemble Empirical Mode Decomposition (EEMD), Complete Ensemble Empirical Mode Decomposition with Adaptive Noise (CEEMDAN), Kalman filter, Savitski-Golay filter, etc., are effective in eliminating noise in the field of signal processing. Explosion signals, particularly those that occur underwater, are a unique type of non-stationary signal that changes its frequency suddenly and in a short amount of time. EMD and its advanced algorithms, such as EEMD and CEEMDAN, have been applied by many scientists to denoise explosion signals. Sun et al. [7], Peng et al. [8], Liu and Peng [9] studied to establish a model denoising the blasting vibration. Research of V. T. Lam et al. [6] studied noise reduction of shockwave pressure signal induced by underwater explosions. The authors admitted that the proposed denoising models are only suitable for certain types of signals in the research, other types of signals still need further study. It is uncontroversial that these studies obtained remarkable results, though. Especially, the study [6] effectively denoised the shockwave pressure signal induced by underwater explosions with a combination algorithm called EMD-CEEMDAN. However, there is a singular jump that occurred in the pressure drop form of explosion signals in this study, this is the reason that the results lack comparisons between the denoised signal and the theoretical pressure drop law.

This article studies the Kalman-EMD combined algorithm for processing the shockwave pressure signal when detonating an explosives charge A-IX-2 in an infinite underwater environment. The denoising model is fine-tuned by the theory of blast wave propagation underwater, the obtained result is the significant elimination of high-frequency noise, and the signal is transformed into a typically smooth explosion signal, close to the theoretical law of pressure drop [10]. Besides, the typical characteristics of blasting parameters such as the peak pressure p_{max}, the positive phase duration τ^+, and the impulse I^+ are also optimized to be closer to theoretical law than calculated values from

the original signal, notwithstanding a tiny trade-off about the error of I^+. In addition, other parameters such as I^- and τ^- can also be extracted.

2. Noise reduction algorithms

This article uses the main algorithm called Kalman filter [11-13] along with a part of the EMD-CEEMDAN algorithm presented in the document [6], which are combined into an algorithm called Kalman-EMD.

The Kalman filter is among the most significant and popular estimation algorithms. The Kalman filter algorithm depends on the rule of a system to predict a priori of a new state and also depends on an actual measurement value to adjust and make a more accurate value of this state. The operation of the Kalman filter is described in the following figure below:

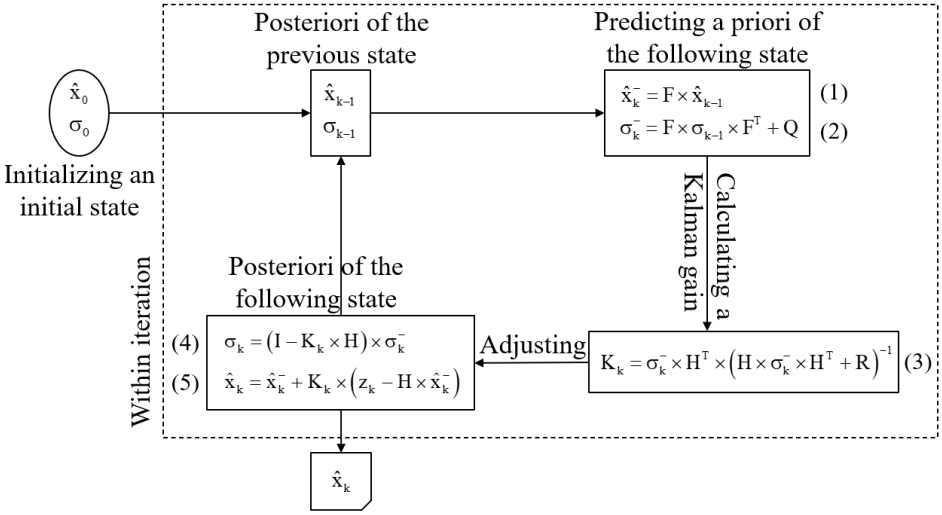

Fig. 1. Flow chart of the Kalman filter.

In Fig. 1, F is the state transition matrix from the previous step k-1 to the current step k; H is the observation matrix that converts the state of measurement space into that of the observation space; Q and R are the system noise, and the measurement noise, respectively; $\hat{x}$ indicates the value of a state estimate; σ is an estimated error variance; K is a Kalman gain; z is an actual observation of a state; subscripts consisting of "k", "k-1", "-" indicate a current state, a previous state and an estimated priori, respectively; quantities without subscript "-" are considered as posterior ones.

The Kalman gain is a key component of the Kalman filter algorithm, it is used to determine how much the new measurement data should be trusted relative to the prediction, a high Kalman gain indicates that the measurement values should be more trusted than that of prediction, and a low Kalman gain indicates vice versa.

3. Experiments on site

The layout diagram and actual photos of the field experiment, including the location of the explosive charge and the sensor, are shown in Fig. 2 as follows:

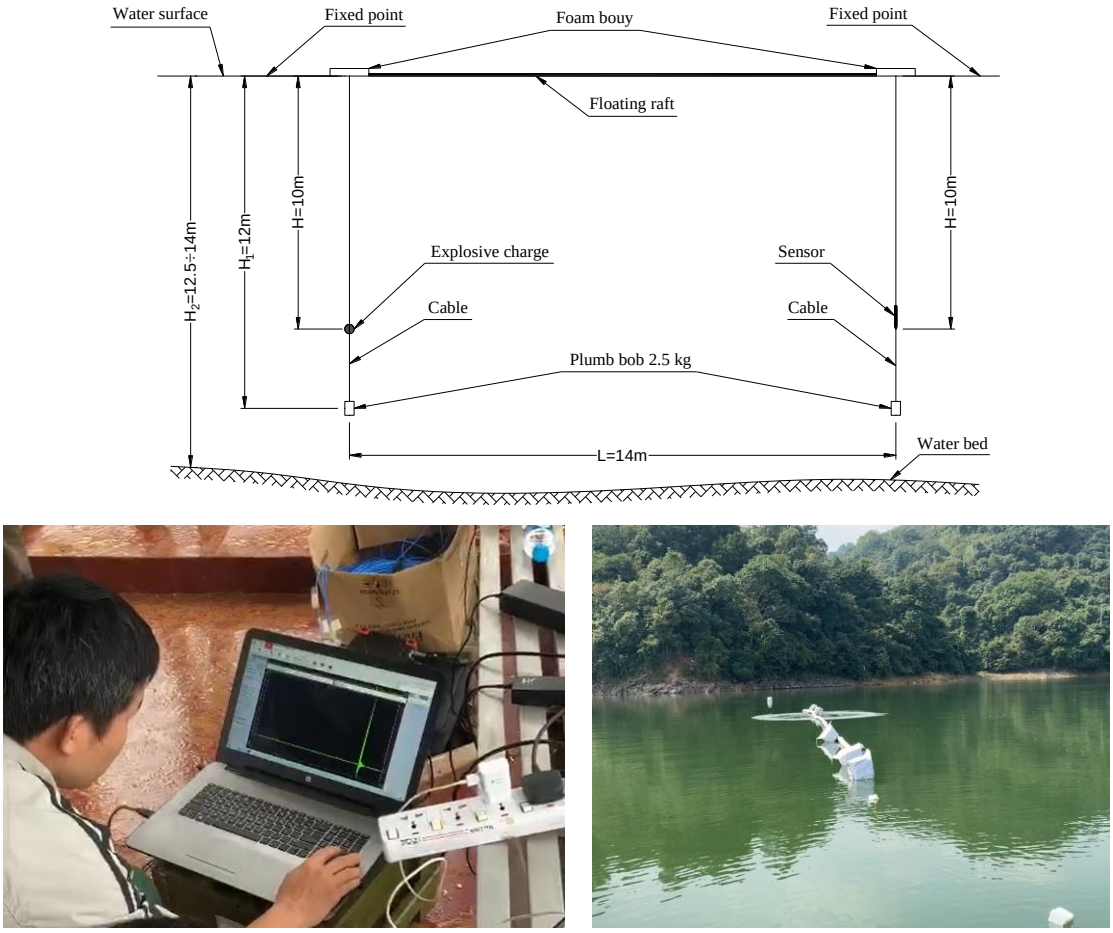

Fig. 2. The layout diagram and actual photos of the field experiment.

In Fig. 2, the floating raft is made from dry bamboo sticks, tied into bundles, ensuring a straightness and length of 18 m. To increase the buoyancy of the raft, foam bars with a cross-section of (10×10) cm are added along the length of the bamboo bundle; at the locations where explosives and sensors are hung on the floating raft, foam floats with the size of (30×30×30) cm are attached. The floating raft is fixed at both ends with cables connected to fixed landmarks on the shore. The explosive charge and the sensor are suspended by steel cables with ϕ3 mm diameter; a 2.5 kg weight is suspended at the bottom end of the cable to tension the hanging rope, ensuring it is not skewed by the water flow. This hanging method is also proposed by PCB manufacturer in their installation and operating manual. The meter is arranged on the boat which is anchored at a position of

50 m far from the foam buoys, in the opposite direction; the detonating electrical wire and sensor wires are connected to the boat.

The sensors used in this experiment are the type of underwater blast sensor 138A05 of the PCB Piezotronics manufactures. The measured data is obtained by a multichannel portable measurement instrument DEWE-3020. Similar to the document [6], a suitable sampling frequency of 200 kHz is chosen. The depth of the experimental area is measured by a Hondex PS-7 portable depth sounder and a measuring tape. The distance is measured by a Nikon laser rangefinder and a measuring tape. The explosive charge used in this experiment weighs 184 grams, including the detonator, which is made from A-IX-2, with the heat of explosion being 1540 kcal/kg, and the explosive density being 1.7 g/cm^3.

The experiment area was selected carefully, it was a tidal area possessing silent water flow and also checked by divers to ensure experimental conditions close to the model described in Fig. 2. Then, a total of 6 underwater explosions were carried out. The most important in these experiments is to ensure all the blasting parameters such as the mass, the size of explosives, and the depth of explosive placement meet the blasting conditions of an infinite medium, allowing the phenomenon of deep underwater explosion, where the effects of the waterbed and water surface do not exist. These conditions are tested through 2 coefficients corresponding to water surface influence k_m and waterbed influence k_d as the following Table 1:

Table 1. Calculated results of k_m and k_d

Equations for k_m and k_d [1, 2]	**Results**
$k_m = \dfrac{0.314\left(\dfrac{H}{r_0}\right)^{2.3}\left(1+4.2\dfrac{h}{H}\right)}{\dfrac{R}{r_0}\sqrt{1-\left(\dfrac{H-h}{r}\right)^2}}$ (6)	$k_m = 1768 > 1$
$k_d = \begin{cases} \dfrac{0.314\left(\dfrac{H_1}{r_0}\right)^{2.3}\left(1+4.2\dfrac{h_1}{H_1}\right)}{\dfrac{r}{r_0}\sqrt{1-\left(\dfrac{H_1-h_1}{R}\right)^2}}; \dfrac{H_1}{r_0} \geq \left(\dfrac{3.22}{\tan\beta^*}\right)^{0.77} \\ \dfrac{H_1}{r_0\tan\beta^*\sqrt{1-\left(\dfrac{H_1-h_1}{R}\right)^2}}\left[1+\dfrac{\dfrac{h_1}{r_0}}{2\left(\dfrac{H_1}{r_0\tan\beta^*}\right)^{0.435}-\dfrac{H_1}{r_0}}\right]; \dfrac{H_1}{r_0} \leq \left(\dfrac{3.22}{\tan\beta^*}\right)^{0.77} \end{cases}$ (7)	$k_d = 7232 > 1$

In Table 1, r is the distance from the explosive center to the waterbed, averaging equal to 2.2 (m); R is the distance from the explosive center to the sensor, equal to

14 (m); r_0 is the radius of explosives, $r_0 = 0.035$ (m); H and h are respectively the distance from the water surface to the explosive center and the interested point, equal to 10 (m) and 10 (m); H_1 and h_1 are the distance from the waterbed to the explosive center and the interested point, equal to 5 (m) and 5 (m) respectively; β^* is the critical angle that reflection coefficient equals 0, chosen as 22^o.

As shown in Table 1, the results indicate that both k_m and k_d are much greater than 1, meaning that the blasting conditions of an infinite medium are satisfied, and the location, where the sensor is placed, is not affected by the water surface and the waterbed.

4. Criteria for evaluating the noise reduction effectiveness

Because the blasting conditions of an infinite medium are satisfied, the efficiency of noise reduction is directly evaluated by theoretical blasting parameters such as the peak pressure of wavefront p_{max}, the positive phase duration τ^+, and the impulse I^+. These values, which are calculated from the initial signal, the denoised signal, and the blasting theory, are then compared to each other, leading to the final evaluation.

Transform the experimental formula calculating the maximum pressure on the front of shockwave p_{max} [10, 14] when blasting in an infinite water environment considering the conversion to TNT explosive equivalent, and its time course $p(t)$ as follows:

$$p_{max} = 52.3 \times \left(\frac{\sqrt[3]{k_T \times C}}{R} \right)^{1.13} \tag{8}$$

$$p(t) = P_{max} \times e^{-\frac{t}{\theta}} \tag{9}$$

where p_{max} is the peak pressure (MPa); k_T is the TNT explosive equivalent; C is the mass of the explosive (kg); R is the distance from the explosive to the sensor (m); t is the time (ms); θ is the time exponential coefficient (ms). θ is calculated through the following equation:

$$\theta = 0.093 \times \sqrt[3]{k_T \times C} \left(\frac{\sqrt[3]{k_T \times C}}{R} \right)^{-0.22} \tag{10}$$

The formula calculating the time constant for a spherical explosive [1, 2]:

$$\frac{a_1 \times \vartheta}{r_0} = 1.4 \times \left(\frac{r}{r_0} \right)^{0.24} \tag{11}$$

where a_1 is the acoustic velocity in the water, $a_1 = 1500$ (m/s); r_0 is the radius of spherical explosive (m) - the explosive of 184 grams A-IX-2 with the heat of explosion as 1540 (kcal/kg) can be transformed into a spherical equivalent explosive that has a radius

of 0.035 (m) through the equation $r_0 = \sqrt[3]{k_T.C}/18.7$; r is the distance from the center of the explosive to the interested point (m).

From equation (11), the time constant is derived, $\vartheta = 1.380 \times 10^{-4}$.

Meanwhile, the positive phase duration can be approximately taken as follows [1, 2]: $\tau^+ \cong 5 \times \vartheta = 6.898 \times 10^{-4}$ (s).

The impulse of the positive phase can be calculated by the following equation:

$$I_+ = \int_0^{\tau^+} \left(p_{(t)} - \gamma_n.h_n \right) dt = \left(p_{\max} - \gamma_n.h_n \right).\vartheta.\left(1 - e^{-\frac{\tau^+}{\vartheta}} \right) \quad (12)$$

where γ_n is the density of water, γ_n = 981 (N/m^3); h_n is the depth of explosive placement, h_n = 10 (m); p_{max} in this equation has to be transformed into (N/m^2); other parameters are as equations (8), (9), (10), (11).

The blasting parameters calculated from equations (8), (10), (11), (12) are summarized in Table 2 as follows:

Table 2. The summary table of theoretical underwater blasting parameters

Explosive type	**TNT equivalent**	**Mass (kg)**	**Distance from the sensor (m)**	**p_{max} (MPa)**	**Θ (ms)**	**τ^+ (ms)**	**I_+ (N.s/m^2)**
A-IX-2	1.54	0.184	14	1.649	0.120	0.690	224.626

5. Signal analysis and processing

5.1. The original signal of underwater blast wave pressure

The measured signal of shockwave pressure induced by 6 underwater explosions as aforementioned experimental conditions are similar, Fig. 3 shows the signal of the 1st blasting with the 1st incident wave is magnified on the upper right (a) and its segmented version (b), considered as a typical signal.

Technically, the original signals are split into three segments. The first and the second segments only need to show the signal trend, so the EMD algorithm is applied to extract its residue and the beginning point of the pressure jump. The third segment is processed by a Kalman filter assuming that the measured peak is correct, it means that the initialized initial value of the posterior state estimate ($\hat{x}_{k-1}$) equals the peak pressure p_{max}, and the posterior error variance (σ_{k-1}) of the initial state equals 0. Then, the first and last points of the 2nd segment are assigned by the last and the first points of Segment 1 and Segment 3, respectively.

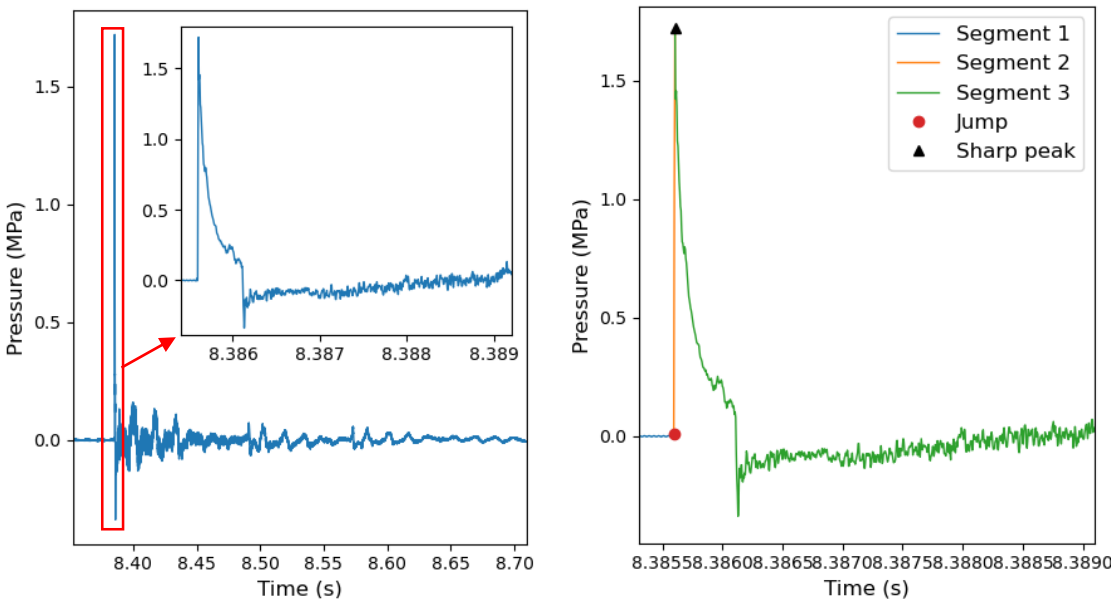

a) Typical signal *b) Typical segmented signal*

Fig. 3. The typical signal of underwater blast wave pressure.

5.2. Parameter initialization of the Kalman filter to fine-tune the pressure drop signal line and denoise the Segment 3

The pressure of a certain point in the water environment, changing over time can be described by the approximate equation [1, 2] as follows:

$$\frac{p - p_n}{p_n} = \frac{p_\phi - p_n}{p_n} \times e^{-\frac{t}{\vartheta}} \tag{13}$$

where t is the time from the start of the impact to the moment under consideration; p is the pressure on the shock wave front at the considered time; p_ϕ is the maximum pressure on the shock wave front; p_n is the pressure of the surrounding water environment; ϑ is the time constant, determined according to (11).

Due to $p_n \ll p_\phi$, for simplicity, equation (13) can be rewritten as follows:

$$p = p_\phi \times e^{-\frac{t}{\vartheta}} \tag{14}$$

Consider any two continuous states in the pressure drop, which are called State 1 and State 2, peak pressures are p_1 and p_2, respectively:

$$p_1 = p_\phi \times e^{-\frac{t}{\vartheta}} \text{ and } p_2 = p_\phi \times e^{-\frac{t+\Delta t}{\vartheta}} \tag{15}$$

From equation (15), get the ratio of p_2/p_1 as follows (16):

$$\frac{p_2}{p_1} = e^{-\frac{t+\Delta t}{\vartheta}+\frac{t}{\vartheta}} = e^{-\frac{\Delta t}{\vartheta}} = e^{-\frac{\Delta t \times a_1}{1.4 \times r^{0.24} \times r_0^{0.76}}} = e^{-\frac{\frac{1}{200000} \times 1500}{1.4 \times 14^{0.24} \times 0.03^{0.76}}} = e^{-0.041} \quad (16)$$

where parameters are as equation (11).

Hence, the following peak pressure is estimated based on the previous peak pressure, so the state transition process for the pressure drop area is that $F = e^{-0.041}$. On the other hand, because the transition process of the following sequential area is unknown, the state transition process returns to 1.

The system noise variance Q is chosen as the specification of sensor W138A05: The measured maximum value for each explosion is p_{max} MPa, with the error of 2%FS. Hence, it can be considered that the most inaccurate case has the highest variance, so $Q = \left(p_{\max} \times 0.02 \right)^2$.

The observation error H is chosen as 1 because the output is the values of pressure, which need to be measured.

The most difficult task in the algorithm is the selection of the measurement noise variance R. This parameter needs to vary for each signal. This article develops a procedure to choose a suitable value of R as follows: R must be as small as possible, and both the errors of impulse I^+ and the error of positive phase duration τ^+ have to be small enough, but τ^+ is a priority. Consequently, the suitable value is the intersection between errors of impulse and errors of positive phase duration. The results are shown in Fig. 4 below.

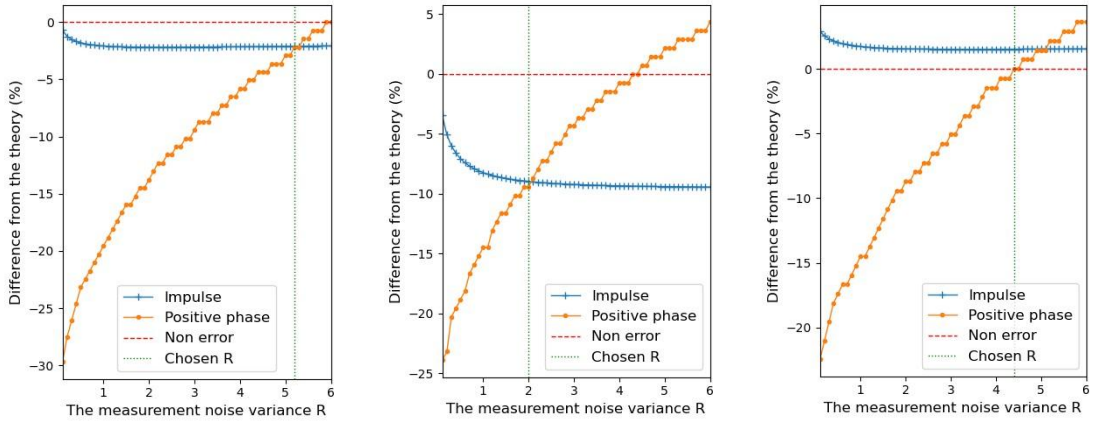

a) Signal 1, Chosen R = 5.2 *b) Signal 2, Chosen R = 2.0* *c) Signal 3, Chosen R = 4.4*

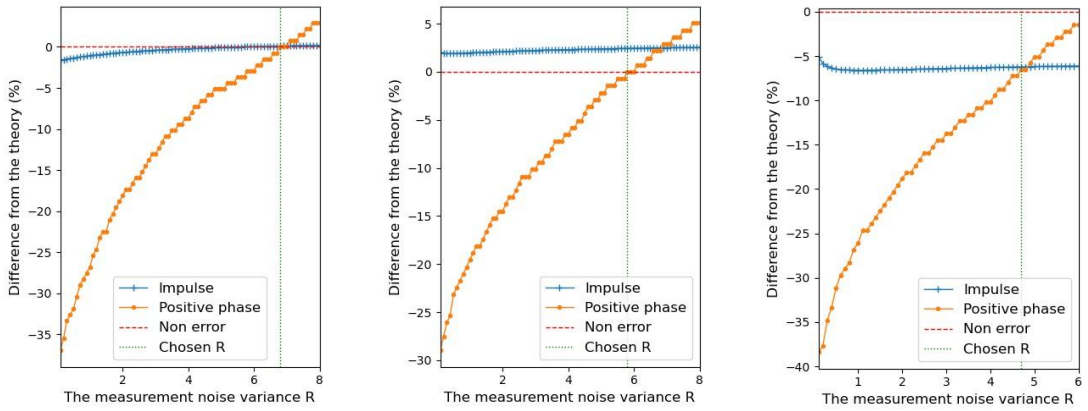

d) Signal 4, Chosen R = 6.8 *e) Signal 5, Chosen R = 5.8* *f) Signal 6, Chosen R = 4.7*

Fig. 4. Error correlations of impulse and positive phase duration between Segment 3 of the 6 denoised signals and the theory.

The Kalman filter parameters for the case of this study are shown in Fig 5 below.

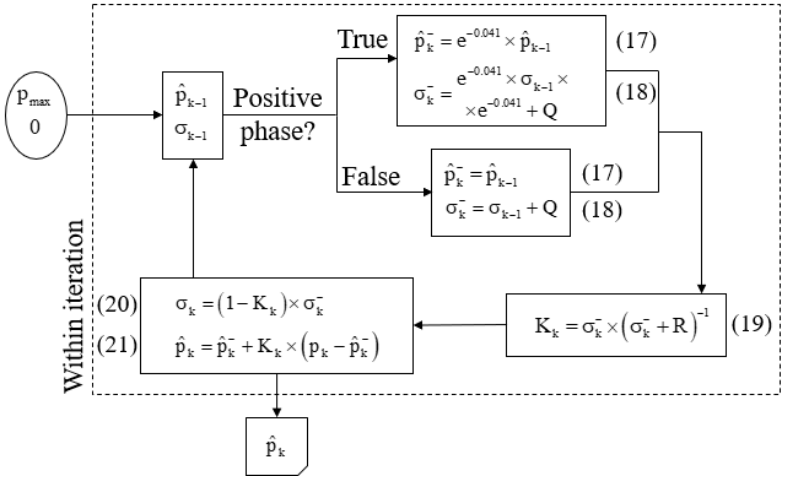

Fig 5. The Kalman filter for the shockwave pressure signal of an underwater explosion.

In Fig. 5, the general system state *x* is replaced by values of pressure *p*, other parameters, and subscripts are similar to that of Fig. 1.

5.3. The denoising results and evaluations

The result of denoising underwater blast waves when applying the Kalman-EMD algorithm for a typical signal is shown in Fig. 6. The signal of the incident wave in the red frame is magnified and separately shown in the upper right of the figure. It can be seen intuitively that noises in the original signal are significantly eliminated. At the same time, the general waveform is still preserved, looking quite close to the pressure drop law of underwater explosion theory [10]. Results for the 5 remaining signals are similar.

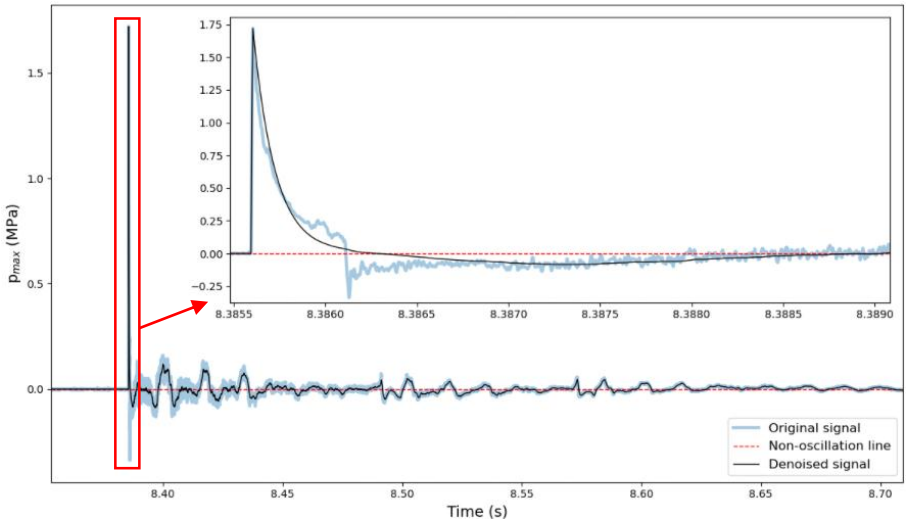

Fig. 6. The denoising result visualization of the typical signal.

To further analyze the effectiveness of the denoising process, the characteristic parameters of the explosion in the water environment are calculated from the original signal and the denoised signal, respectively, and then compared with the calculation results from the theory. In particular, the peak pressure parameter p_{max} is easily found from the signal with some available functions in Python, other parameters such as the positive phase duration τ^+ and the impulse I^+ of the explosion are illustrated in Fig. 7, calculated by the Riemann integral.

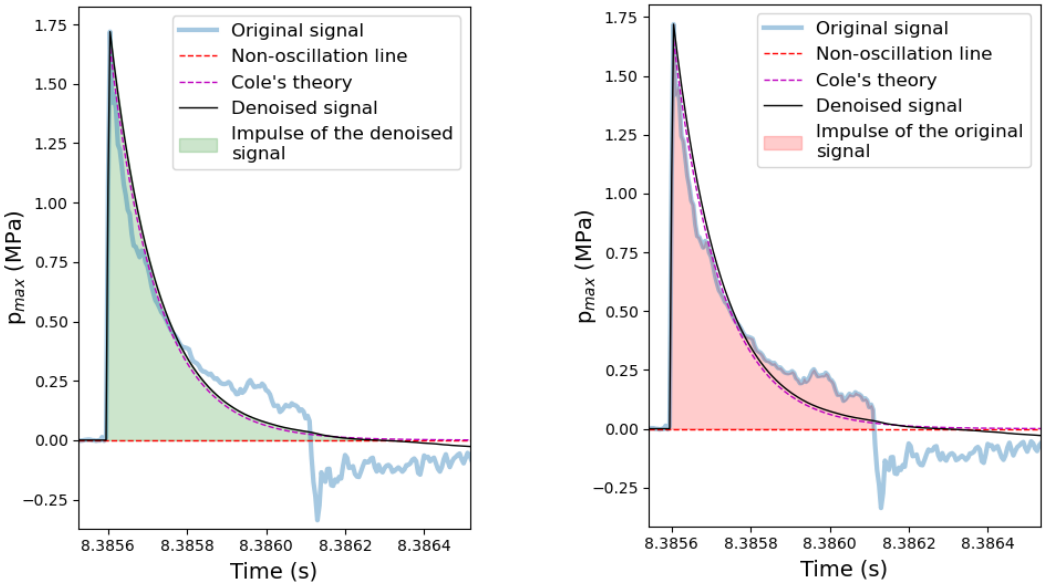

(a) *(b)*

Fig. 7. Illustrations of I^+ and τ^+ of the original signal (a) and the denoised signal (b).

The positive phase duration is determined as the total sampling points calculated from where the pressure jump occurred to the first zero-crossing point and then multiplied by the sampling cycle. The calculated results are summarized in the following table.

Table 3. The summary table of underwater explosion parameters

No.	**The original signal and difference compared with the theory**			**The denoised signal and difference compared with the theory**			**Obtained values from theoretical equations (8), (12)**		
	p_{max} (MPa)	Impulse I^+ ($N.s/m^2$)	τ^+ (ms)	p_{max} (MPa)	Impulse I^+ ($N.s/m^2$)	τ^+ (ms)	p_{max} (MPa)	Impulse I^+ ($N.s/m^2$)	τ^+ (ms)
1	1.669 1.21%	218.788 2.60%	0.465 32.61%	1.669 1.21%	211.557 5.82%	0.670 2.90%	1.649	224.626	0.690
2	1.551 5.94%	220.840 1.69%	0.505 26.81%	1.551 5.94%	196.727 12.42%	0.625 9.42%			
3	1.720 4.31%	225.408 0.35%	0.520 24.64%	1.720 4.31%	219.446 2.31%	0.690 0.00%			
4	1.699 3.03%	212.993 5.18%	0.415 39.86%	1.699 3.03%	216.361 3.68%	0.685 0.72%			
5	1.740 5.52%	221.384 1.44%	0.475 31.16%	1.740 5.52%	221.409 1.43%	0.690 0.00%			
6	1.621 1.70%	210.932 6.10%	0.405 41.30%	1.621 1.70%	202.556 9.83%	0.640 7.25%			
Average	3.62%	2.89%	32.73%	3.62%	5.91%	3.38%	0.00%	0.00%	0.00%

By qualitative analysis of Fig. 7 combined with quantitative analysis of Table 3, it can be seen that the pressure drop section of the denoised signal almost coincides with the theoretical pressure drop law [10]. Because the study assumes that the measured maximum pressure is accurate to simplify the Kalman filter algorithm, the errors of p_{max} in both the original and the denoised signals are the same, averaging about 3.62% compared to the theory. The errors of I^+ for the original and the denoised signals, respectively compared to the theory, insignificantly rise from about nearly 3% to nearly 6%. However, corresponding τ^+ parameters remarkably decrease from an average of 32% to about a little more than 3%. In terms of technical problems, a small trade-off of about

3% for one parameter, exchanging for more accuracy of another parameter up to 30%, then this trade-off seems to be acceptable.

Additionally, the parameters I^- and τ^- can be extracted from denoised signals, which cannot be done in the original signals. The results for the negative phase of 6 experimental signals are shown in Table 4, along with a typical intuitive illustration in Fig. 8.

Table 4. The summary table for the negative phase of underwater explosions

No.	Impulse I^- ($N.s/m^2$)	τ^- (ms)
1	-108.172	2.635
2	-129.749	2.590
3	-120.627	2.745
4	-94.705	2.640
5	-111.447	2.765
6	-97.061	2.645

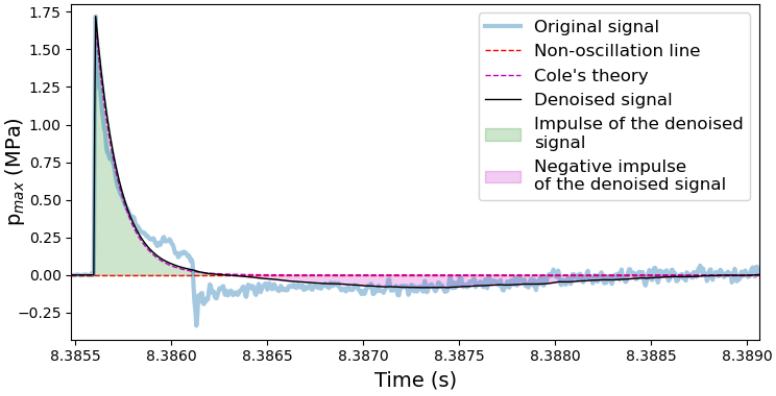

Fig. 8. Negative impulse illustration of a typical denoised signal.

6. Conclusion and recommendation

A measured signal of an underwater explosion is often disturbed by noise sources surrounding the environment, causing waveform distortion. This article develops the Kalman-EMD algorithm combining the Kalman filter and empirical mode decomposition for processing this signal type. The state transition parameter F of the Kalman filter is applied differently for two stages, corresponding to the positive and the negative phases of signals. The results when using the algorithm for 6 underwater explosion signals show that the signal form becomes smoother, close to the pressure drop law of Cole's theory, meaning that the noise is significantly eliminated. There has been a small trade-off of about 3% for the error of the negative impulse I^+ compared to the theory in detail, the error of the positive duration τ^+ decreases a huge number by about 30%, though. The algorithm also helps extract information about the negative phase from signals, which is almost impossible for original signals.

The article is considered one of the preliminary studies about denoising the shockwave pressure signal of underwater explosions. The results show that positive phases of signals are processed fairly well. Quantitative data is close to theory, showing the reliability of the denoising model for this phase. Besides, although negative phases can be extracted, further studies are still necessary to obtain the final confirmation.

References

[1] Hồ Sĩ Giao, Đàm Trọng Thắng, Lê Văn Quyển, Hoàng Tuấn Chung, *Nổ hóa học lý thuyết và thực tiễn*. Nxb Khoa học tự nhiên và Công nghệ, 2010.

[2] Đàm Trọng Thắng, Bùi Xuân Nam, Trần Quang Hiếu, *Nổ mìn trong ngành mỏ và công trình*. Nxb Khoa học tự nhiên và Công nghệ, 2015.

[3] Đàm Trọng Thắng và nnk, Đề tài cấp Quốc gia, mã số: 32/18-C-ĐTĐL.CN.CNC, 2022.

[4] Đàm Trọng Thắng, Trần Đức Việt, "Sự biến đổi của sóng nổ tại mặt phân cách giữa môi trường nước và môi trường nước chứa bóng khí", *Tạp chí Nghiên cứu khoa học và Công nghệ quân sự*, Số 70, 2020. DOI: 10.54939/1859-1043.j.mst.70.2020.139-145

[5] Đàm Trọng Thắng, Trần Đức Việt, "Nghiên cứu ảnh hưởng của màn chắn bóng khí đến trường sóng nổ lan truyền trong môi trường nước", *Tạp chí khoa học kỹ thuật Mỏ - Địa chất*, Tập 62, Kỳ 5, 2021. DOI: 10.46326/JMES.2021.62(5).09

[6] V. T. Lam, D. T. Thang, T. D. Viet, "Denoising the shockwave pressure signal of underwater explosion based on EMD-CEEMDAN in consideration of the signal curve curvature", *Journal of Science and Technique, Section on Special Construction Engineering*, Vol. 06, No. 02, 2023. DOI: 10.56651/lqdtu.jst.v6.n02.745.sce

[7] M. Sun, L. Wu, C. Li, Q. Yuan, Y. Zhou, X. Ouyang, "Smooth model of blasting seismic wave signal denoising based on two-stage denoising algorithm", *Journal of Geosystem Engineering*, 2020. DOI: 10.1080/12269328.2020.1778543

[8] Y. Peng, Y. Liu, C. Zhang, L. Wu, "A Novel Denoising Model of Underwater Drilling and Blasting Vibration Signal Based on CEEMDAN", *Arabian Journal for Science and Engineering*, 2021. DOI: 10.1007/s13369-020-05274-z

[9] Z. Liu, Y. Peng, "Study on Denoising Method of Vibration Signal Induced by Tunnel Portal Blasting Based on WOA-VMD Algorithm", *Journal of Applied Sciences*, 2023. DOI: 10.3390/app13053322

[10] R. H. Cole, *Underwater explosions*. Princeton University Press: Princeton, NJ, USA, 1948.

[11] R. E. Kalman, "A new approach to Linear Filtering and Prediction problems", *Journal of Basic Engineering*, 1960. DOI: 10.1115/1.3662552

[12] G. Welch, G. Bishop, *An introduction to the Kalman filter*. University of North Carolina, 2006.

[13] https://www.kalmanfilter.net/default.aspx

[14] R. Kicínski, B. Szturomski, "Pressure Wave Caused by Trinitrotoluene (TNT) Underwater Explosion - Short Review", *Journal of Applied Sciences*, 2020. DOI: 10.3390/app10103433

PHÁT TRIỂN THUẬT TOÁN KẾT HỢP KALMAN-EMD ĐỂ XỬ LÝ TÍN HIỆU SÓNG XUNG KÍCH DO NỔ LAN TRUYỀN TRONG MÔI TRƯỜNG NƯỚC

Vũ Tùng Lâm[1], Trần Đức Việt[2], Bùi Ngọc Lâm[3], Đàm Trọng Thắng[1]

[1]*Viện Kỹ thuật công trình đặc biệt, Trường Đại học Kỹ thuật Lê Quý Đôn, Hà Nội, Việt Nam*

[2]*Tổng cục Công nghiệp quốc phòng, Hà Nội, Việt Nam*

[3]*Nhà máy X28, Hải Phòng, Việt Nam*

Tóm tắt: Dữ liệu đo trong các thí nghiệm có triển khai các cảm biến đo áp suất nổ dưới nước luôn bị nhiễu, biểu hiện ở các đỉnh răng cưa của dạng tín hiệu thu được. Ngoại trừ áp suất đỉnh P_{max}, các tham số khác của một vụ nổ dưới nước như xung nén I^+, thời gian pha nén τ^+, xung dãn I^-, thời gian pha dãn τ^- là rất khó hoặc gần như không thể trích xuất từ những tín hiệu này. Bài báo nghiên cứu phát triển một thuật toán Kalman-EMD là sự kết hợp của bộ lọc Kalman và phân tách dạng thực nghiệm để xử lý loại tín hiệu nổ này. Thuật toán được áp dụng vào 6 bộ dữ liệu đo áp suất sóng nổ dưới nước bằng cảm biến PCB W138A05 với cùng một điều kiện kích nổ lượng thuốc 184 gam A-IX-2, kết quả cho thấy nhiễu trong tín hiệu được loại bỏ đáng kể. Đối với các tham số nổ có thể so sánh được với lý thuyết như I^+ và τ^+, mặc dù có sự đánh đổi nhỏ về sai số của I^+ khi tăng từ khoảng 3% lên 6%, nhưng sai số τ^+ lại giảm đáng kể từ trên 30% xuống còn khoảng 3%. Đặc biệt, các thông tin khác như I^- và τ^- có thể trích xuất được từ tín hiệu sau xử lý nên sự đánh đổi này có thể chấp nhận được. Như vậy, thuật toán này có thể được sử dụng để xử lý khử nhiễu, trích xuất các tham số nổ từ tín hiệu thu được khi kích nổ một lượng thuốc dưới nước.

Từ khóa: *Nổ dưới nước; khử nhiễu; phân tách dạng thực nghiệm (EMD); bộ lọc Kalman.*

Received: 27/03/2024; Revised: 20/06/2024; Accepted for publication: 28/06/2024

❑